tvst

Article

A Mouse Model of Proliferative Vitreoretinopathy Induced by Intravitreal Injection of Gas and RPE Cells

Alison Heffer[1], Victor Wang[2], Jayanth Sridhar[3], Steven E. Feldon[4,5], Richard T. Libby[6,7], Collynn F. Woeller[8,*], and Ajay E. Kuriyan[9–11,*]

[1] Flaum Eye Institute, University of Rochester, Rochester, NY, USA
[2] Flaum Eye Institute, University of Rochester, Rochester, NY, USA
[3] Bascom Palmer Eye Institute, University of Miami Miller School of Medicine, Miami, FL, USA
[4] Flaum Eye Institute, University of Rochester, Rochester, NY, USA
[5] Center for Visual Sciences, University of Rochester, Rochester, NY, USA
[6] Flaum Eye Institute, University of Rochester, Rochester, NY, USA
[7] Center for Visual Sciences, University of Rochester, Rochester, NY, USA
[8] Flaum Eye Institute, University of Rochester, Rochester, NY, USA
[9] Retina Service, Wills Eye Hospital, Thomas Jefferson University, Philadelphia, PA, USA
[10] Flaum Eye Institute, University of Rochester, Rochester, NY, USA
[11] Center for Visual Sciences, University of Rochester, Rochester, NY, USA

Correspondence: Ajay E. Kuriyan, 840 Walnut Street, Suite 1020, Philadelphia, PA 19107, USA. e-mail: ajay.kuriyan@gmail.com

Received: January 30, 2020
Accepted: April 4, 2020
Published: June 5, 2020

Keywords: proliferative vitreoretinopathy; mouse; retinal detachment; contractile membranes

Citation: Heffer A, Wang V, Sridhar J, Feldon SE, Libby RT, Woeller CF, Kuriyan AE. A mouse model of proliferative vitreoretinopathy induced by intravitreal injection of gas and RPE cells. Trans Vis Sci Tech. 2020;9(7):9, https://doi.org/10.1167/tvst.9.7.9

Purpose: Develop a reproducible proliferative vitreoretinopathy (PVR) mouse model that mimics human PVR pathology.

Methods: Mice received intravitreal injections of SF_6 gas, followed by retinal pigment epithelial cells 1 week later. PVR progression was monitored using fundus photography and optical coherence tomography imaging, and histologic analysis of the retina as an endpoint. We developed a PVR grading scheme tailored for this model.

Results: We report that mice that received gas before retinal pigment epithelial injection developed more severe PVR. In the 1×10^4 retinal pigment epithelial cell group, after 1 week, 0 of 11 mice in the no gas group developed grade 4 or greater PVR compared with 5 of 13 mice in the SF_6 gas group ($P = 0.02$); after 4 weeks, 3 of 11 mice in the no gas group developed grade 5 or greater PVR compared with 11 of 14 mice in the SF_6 gas group ($P = 0.01$). We were able to visualize contractile membranes both on the retinal surface as well as within the vitreous of PVR eyes, and demonstrated through immunohistochemical staining that these membranes expressed fibrotic markers alpha smooth muscle actin, vimentin, and fibronectin, as well as other markers known to be found in human PVR membranes.

Conclusions: This mouse PVR model is reproducible and mimics aspects of PVR pathology reported in the rabbit PVR model and human PVR. The major advantage is the ability to study PVR development in different genetic backgrounds to further elucidate aspects of PVR pathogenesis. Additionally, large-scale experiments for testing pharmacologic agents to treat and prevent PVR progression is more feasible compared with other animal models.

Translational Relevance: This model will provide a platform for screening potential drug therapies to treat and prevent PVR, as well as elucidate different molecular pathways involved in PVR pathogenesis.

Introduction

Proliferative vitreoretinopathy (PVR) is a condition that occurs in 5% to 10% of rhegmatogenous retinal detachments, resulting in poor visual outcomes and the need for recurrent surgical interventions.[1–3] A major component of PVR pathophysiology involves migration of retinal pigment epithelial (RPE) cells into the vitreous cavity after a retinal tear.[4–7] Subsequently, the

RPE cells are exposed to growth factors and cytokines that promote proliferation and epithelial–mesenchymal transition (EMT) to fibrotic cells.[4–6] These fibrotic cells with contractile properties are the main component of tractional membranes that form on the surfaces of the retina and within the vitreous which pull on the retina, leading to retinal folds and detachments and eventually damage to underlying photoreceptors.[8–10]

Several in vivo studies attempted to reproduce various aspects of PVR disease progression in different animal systems.[11] Experimental models in animals with larger eyes, including those in nonhuman primates,[12] cats,[13] and pigs[14] have used surgical techniques to promote retinal detachments, followed by injection of different cell types. Because preretinal tractional membranes are commonly found in patients with PVR, many other studies attempted to induce the formation of these PVR membranes and tractional retinal detachments through injection of cells from various sources including RPE cells,[14–17] fibroblasts,[18,19] Müller cells,[20] blood,[21] and macrophages.[22] In most cases, tractional PVR membranes developed within 1 to 4 weeks after injection that were similar to human PVR membranes.[11]

The rabbit PVR model has emerged as the most widely used animal model of PVR. The rabbit eye has a relatively large vitreous cavity and small lens, which allows for the use of human surgical and examination tools.[11] In this model, gas is placed in the vitreous cavity by intravitreal injection to induce a posterior vitreous detachment, followed by a subsequent intravitreal injection of RPE cells.[18,19,23–26] The collapsed vitreous and development of tractional membranes are similar to those seen in human PVR.[18,19,23] A shortcoming of this model is the inability to use genetic manipulation to gain a better understanding of PVR pathophysiology. Furthermore, the cost and space requirements for rabbits, compared with mice, limits the ability to perform experiments with a large sample size.

Although the mouse provides a plethora of genetic tools, it has not been used extensively as a model for PVR, largely owing to its small eye with a large lens and small vitreous relative to other animal models.[27] Currently, the most popular mouse PVR model uses injection of the proteolytic enzyme dispase.[28–31] Although dispase injection may trigger events that lead to PVR formation, such as cells invading the vitreous cavity, retinal folds, and the appearance of intravitreal membranes,[28] the integrity of the retina is severely affected. The dispase enzyme breaks down the retina structure, producing marked hemorrhage, which does not mimic human PVR pathogenesis or progression.

The successful development of a mouse model, using the techniques of gas and RPE injection as used in the widespread rabbit PVR model, would potentially allow the manipulations of genetically identical strains to study in vivo PVR pathogenesis. Additionally, the practicality of using large numbers of animals to evaluate candidate drugs to treat PVR could be tested in a more cost-effective manner, given the lower cost for purchasing and housing mice compared with rabbits. Here, we present a new mouse model of PVR that replicates aspects of the rabbit PVR model (intravitreal gas and RPE injection), with resultant development of preretinal membranes and tractional retinal detachments. We have also established, for the first time in a murine model, a PVR grading scheme. This model and grading scheme can be useful for future testing of different therapeutic molecules to treat and prevent PVR, as well as different genetic backgrounds to further probe PVR pathogenesis.

Methods

Animals

A total of 80 8- to 10-week old female C57BL/6J mice were purchased from Jackson Laboratory (Bar Harbor, ME). All experiments adhered to the ARVO Statement for the Use of Animals in Ophthalmic and Vision Research and were approved by the University Committee of Animal Resources of the University of Rochester.

PVR Induction

Mice were divided into four groups ($n = 15$ for each group, total of 60): (1) no gas/1 $\times$ 10^4 RPE cells injected, (2) SF_6 gas/1 $\times$ 10^4 RPE cells injected, (3) no gas/5 $\times$ 10^4 RPE cells injected, and (4) SF_6 gas/5 $\times$ 10^4 RPE cells injected (Fig. 1). As controls, mice were injected with (1) no gas/PBS (vehicle; $n = 5$) and (2) SF_6 gas/PBS ($n = 15$). After injection, eyes were evaluated by weekly fundus and optical coherence tomography (OCT) imaging at 4 weeks to monitor the development and progression of PVR and assigned a PVR grade (described in Results; Fig. 2). PVR grades were assigned at 1 and 4 weeks. If, during imaging, media opacities prevented a clear view of the retina, the image was deemed ungradable and excluded from this analysis.

SF_6 Injection

Mice were anesthetized with 100 mg/kg ketamine (Par Pharmaceuticals, Chestnut Ridge, NY) and

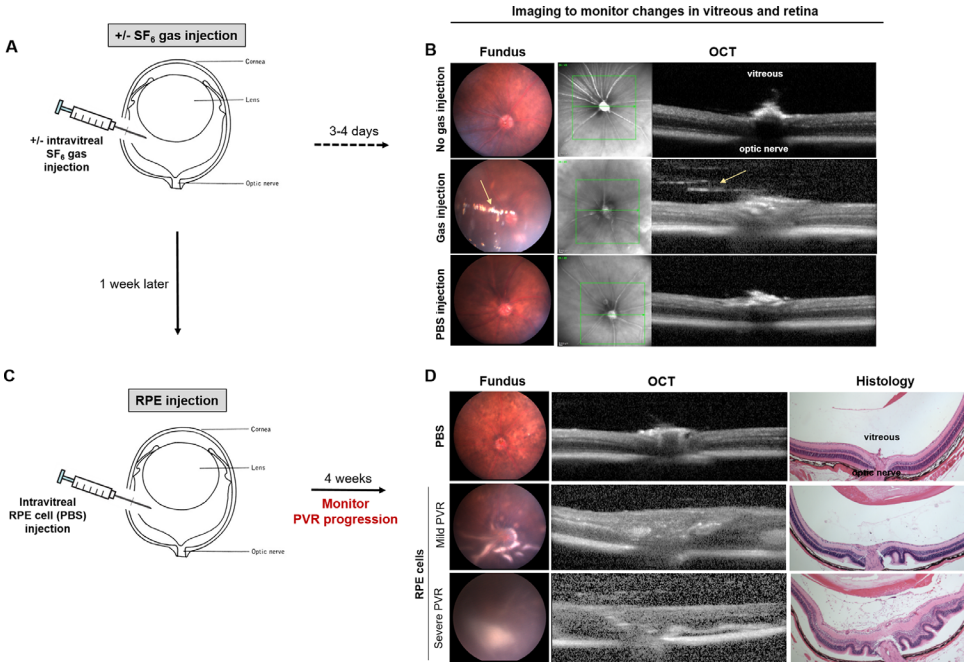

Figure 1. Method for inducing and monitoring PVR in mice. (A) We injected 0.5 µL of 100% SF_6 gas into the vitreous cavity of a subset of mice to induce a posterior vitreous detachment. Another subset of mice did not receive the SF_6 gas injection. (B) In mice that received the intravitreal injection of 100% SF_6 gas, after 3 to 4 days of expansion of the gas in the vitreous cavity results in a posterior vitreous detachment, which can be visualized as reflective spots in a fundus image, which correspond to the vitreous detachment as seen in the OCT image (*yellow arrows*). This was not present in mice that did not receive the intravitreal injection of SF_6 gas and only PBS. (C) One week later, RPE cells were injected into the vitreous cavity of mice that did and did not receive prior intravitreal injection of 100% SF_6 gas. (D) PVR progression was monitored for up to 4 weeks using fundus and OCT imaging, with histologic analysis as an endpoint to confirm the presence of retinal folds and detachments.

10 mg/kg xylazine (Akorn Inc, Lake Forest, IL). The eye being injected was sterilized using a 5% strength betadine/saline solution. An initial puncture through the sclera into the vitreous cavity was performed with a 30G needle, just posterior to the cornea–scleral junction. Subsequently, SF_6 gas (Alcon Laboratories, Ft. Worth, TX) was loaded into an air-tight 10 µL Hamilton syringe (Hamilton, Reno, NV) in which the needle had been removed. The syringe containing SF_6 gas was placed flush against the Hamilton syringe, and gas was pushed into the Hamilton syringe; successful loading of SF_6 gas was indicated by the plunger moving backward. A 33G needle was immediately screwed onto the Hamilton syringe and the plunger was adjusted to 0.5 µL. Immediately afterwards, the 0.5 µL SF_6 gas in the Hamilton syringe was injected into the vitreous cavity through the scleral puncture wound made by the 30G needle, with special care not to damage the lens. The total volume of gas injected was approximately 10% to 13% of the total volume of the vitreous, because the vitreous of the mouse eye has been reported to be 4.4 ± 0.7 µL.[32] After SF_6 injection, the needle was left in the eye for 10 seconds to prevent egress of the gas. Very rarely, a small amount of gas was noted to egress after removal of the needle.

RPE Injection

One week later, RPE cells (ARPE-19, ATCC, Manassas, VA) that had been grown to confluency per the manufacturer's instructions were harvested and counted using a TC-20 Automatic Cell Counter (BioRad, Hercules, CA). RPE cells were resuspended in an appropriate volume of sterile 1× phosphate-buffered saline (PBS) such that 1 µL total cells was used for injection. All RPE cell injections were performed within 1 hour of cell collection. Mice were anesthetized and prepared for injection as described elsewhere in this article. RPE cells were carefully resuspended by gentle agitation and 1 µL was loaded into a 10-µL Hamilton syringe with a 33G needle. To minimize scarring, the scleral site used previously for gas injection the prior week was repunctured using a 30G needle and used for RPE injection. The RPE cells were injected slowly and the needle was left in the eye for 30 seconds after RPE injection to prevent cells from leaking upon needle removal.

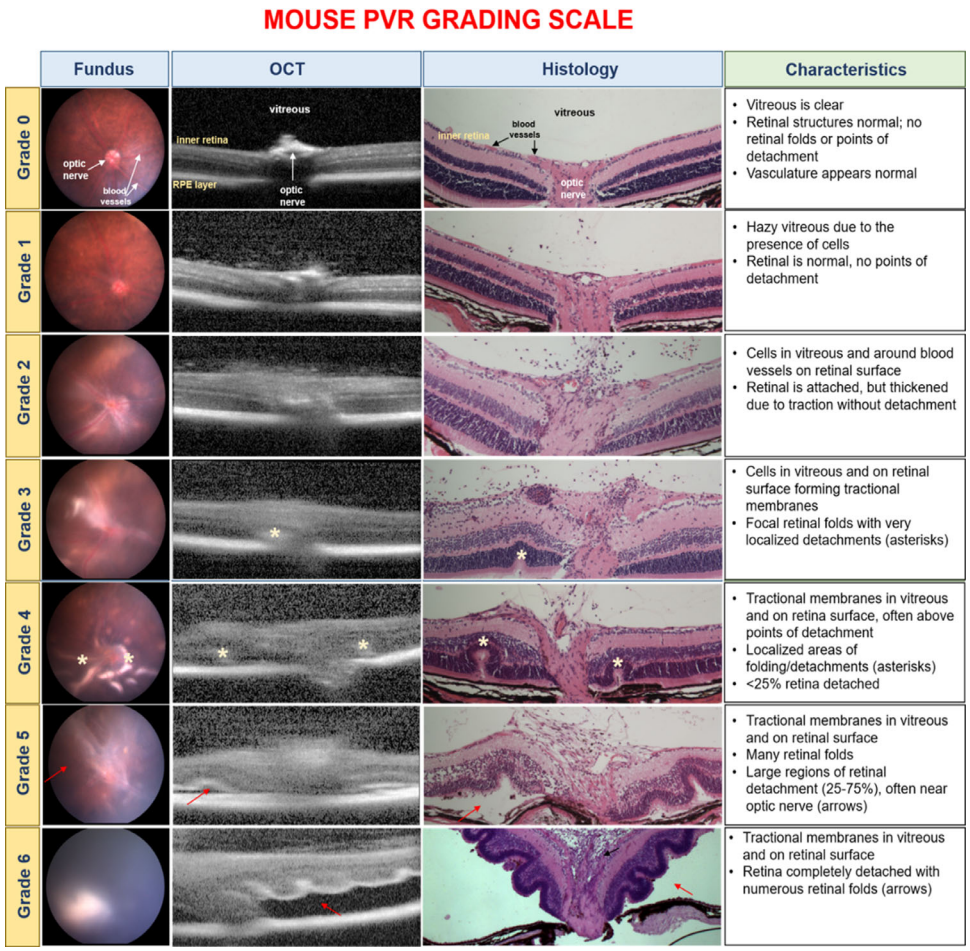

Figure 2. PVR grading scheme for our mouse model of PVR. A PVR grading scheme appropriate for our mouse model was developed from reproducible phenotypes observed in mice after injection with RPE cells. Fundus, OCT and histology (hematoxylin and eosin staining) were used to define aspects of PVR pathology also seen in humans. Characteristics that define each grade are noted and described in the text.

Imaging

Fundus Examination and Photography

PVR development and progression was monitored weekly by fundus imaging. Mice were anesthetized with 100 mg/kg ketamine and 10 mg/kg xylazine. The pupil being imaged was dilated with an ophthalmic solution of phenylephrine 2.5% (Paragon Bioteck Inc, Portland, OR) and tropicamide 1% (Akorn Inc, Lake Forest, IL). The mouse was positioned and GenTeal lubrication gel (Alcon, Fort Worth, TX) was applied to prevent ocular surface drying. Eyes were imaged using the bright-field view of the Micron III (Phoenix Instruments, Naperville, IL). The camera was placed just above the surface of the cornea and images were taken using StreamPix software (Norpix, Montreal, Quebec, Canada).

OCT Retinal Imaging

The presence of vitreous and preretinal cells/membranes and changes in retinal structure were monitored by OCT imaging of the retina. Mice were anesthetized and the pupil was dilated as described elsewhere in this article. The mouse was positioned in a holder with a bite-bar for stabilization of the head, and a small contact lens was placed on the eye to improve the optics and prevent the ocular surface from drying. OCT images were captured using the Heidelberg Spectralis HRA+OCT imaging system (Heidelberg Engineering, Franklin, MA).

Histologic Analysis

Hematoxylin and Eosin Staining

Whole eyes were dissected and immediately fixed in 4% paraformaldehyde for 24 hours at 4°C. Eyes were dehydrated through a series of ethanol and xylene washes before embedding in paraffin. Paraffin sections of 5 to 10 microns were obtained using a Microm HM310 and dried on SuperFrost Plus slides (Fisher, Waltham, MA). For hematoxylin and eosin staining, slides were deparaffinized and rehydrated in a series of

xylenes/ethanol washes and then stained with Mayer's Hematoxylin Solution (Sigma, St. Louis, MO) for 2 to 3 minutes. Slides were then incubated in Bluing Reagent (0.1% sodium bicarbonate) for 30 seconds, rinsed twice in ethanol, and counterstained with Eosin Y (Sigma) for 2 minutes. Extra stain was rinsed with ethanol washes and slides were cleared in xylenes before mounting with Permount (Electron Microscopy Biosciences, Hatfield, PA).

Immunohistochemical Staining

Whole eyes were fixed and sectioned as described elsewhere in this article. Slides were deparaffinized and rehydrated in xylenes and ethanol washes, followed by several washes in water. Antigen retrieval was performed by gently boiling slides in Citrate-based Antigen Unmasking Solution (Vector Laboratories, Burlington, Ontario) for 5 minutes in the microwave. Slides were washed in Tris-buffered saline/Triton-X, blocked in 10% goat serum/1% bovine serum albumin for 2 hours at room temperature, and then incubated overnight in primary antibody diluted in 1% bovine serum albumin/Tris-buffered saline. After rinsing in Tris-buffered saline/Triton-X, slides were incubated in 0.3% H_2O_2 for 15 minutes to block endogenous peroxidase activity before incubation in an horseradish peroxidase-conjugated secondary antibody diluted in 1% bovine serum albumin for 2 hours at room temperature. After washing, slides were stained with diaminobenzidine (Vector Laboratories) until color reaction was visible. Slides were counterstained with hematoxylin, then dehydrated, cleared, and mounted using Permount. All imaging was done on an Olympus BX51 microscope (Olympus, Shinjuku, Tokyo, Japan). Primary antibodies and dilutions used were alpha smooth muscle actin (1:400, rabbit, Abcam, Cambridge, UK), fibronectin (1:500, rabbit, Abcam), vimentin (1:400, rabbit, Cell Signaling Technologies, Danvers, MA), glial fibrillary acidic protein (1:200, rabbit, Cell Signaling Technologies), CD3 (1:200, rabbit, GeneTex, Irvine, CA), and CD20 (1:200, rabbit, LSBio, Seattle, WA). For the secondary antibody, an horseradish peroxidase-conjugated secondary antibody (1:500, goat, Jackson ImmunoResearch, West Grove, PA) was used.

Statistical Analysis

Fundus and OCT images of mice ($n = 15$ for each gas/RPE condition described elsewhere in this article and $n = 20$ for PBS control mice, total $N = 80$) collected at 1 and 4 weeks after RPE injection were independently graded by two retinal specialists (AEK, JS) who were blinded to the experimental conditions at the time of grading. Any grades that differed were discussed and a consensus PVR grade was decided upon. The distribution of grades for each injection group are presented as violin plots and χ^2 analyses were used to compare the severity of PVR grade between the groups.

Results

Intravitreal Injection of 100% SF_6 Gas Induces a PVD in Mice

Injection of 0.5 µL 100% SF_6 gas into the vitreous cavity of 45 of 45 mice (100%, Fig. 1A) resulted in the detachment of the vitreous from the retina near the optic nerve 3 to 4 days after injection, as visualized by fundus and OCT imaging (Fig. 1B, yellow arrows). A posterior vitreous detachment was not present in 30 of 30 (100%) mice who did not receive a gas injection before RPE injection or 5 of 5 (100%) mice who received only PBS injection. We are confident that the reflective band visualized by OCT is the vitreous detachment, because gas creates a characteristic shadowing that was not present in our OCTs. Additionally, we would be able to visualize the gas meniscus using fundus photography if it were in the plane of the OCT that was taken.

Establishing a PVR Grading Scheme Appropriate for Our Mouse Model

There was a proportional increase in the severity and rate of progression of PVR with an increase in the number of RPE cells injected into the vitreous, as seen by fundus and OCT imaging and confirmed by histology. The variation was documented and used to create a grading scheme of PVR severity based on previous grading schemes,[15] but specific to the reproducible phenotypes that we observed in the mouse model (Fig. 2). The grading scheme was designed based off the visual differences observed in the RPE-injected eyes recorded with OCT imaging and histology. Grade 0 PVR was observed in all control eyes (20 of 20, 100%). Fundus and OCT imaging show no anomalies in retinal thickness and appearance, and no cells were detected in the vitreous; histology confirms all layers of the retina appear normal and there are no epiretinal or vitreous contractile membranes. Grade 1 PVR is characterized by a slightly hazy fundus image, which was confirmed by OCT imaging and histology to be due to the presence of RPE cells in the vitreous and on the inner retinal surface. In grade 2 PVR, the RPE cells migrate to the blood vessels on the inner

retinal surface and exert a small degree of traction: the fundus image shows hypopigmented membranes along the retinal blood vessels and the OCT image shows thickening of the retina without detachment. Histology confirms the presence of cells around the vasculature and a thickened retina. Grade 3 PVR is characterized by cells along the vasculature and small pockets of subretinal fluid and/or retinal folds traction, often adjacent to a retinal blood vessel. Fundus photography shows hypopigmented membranes around the retinal vasculature with a focal area of elevation. OCT images and histology demonstrate small pockets of subretinal fluid. In grade 4 PVR, there are multiple focal retinal detachments. These appear as numerous hypopigmented areas deep to the retinal vessels by fundus imaging, which correspond with small pockets of subretinal fluid by OCT. Histology also shows multiple focal areas of retinal detachment, which are in close proximity to tractional membranes on the surface of the retina. Less than 25% of the retina is detached in grade 4 PVR. In grade 5 PVR, there are larger areas of retinal detachment. These areas are visualized by fundus imaging as regions that are elevated and therefore seem to be out of focus. OCT images demonstrate larger pockets of subretinal fluid with traction. Histologic analysis confirms that there are larger regions of detachment; the areas of retinal detachments often occur around the optic nerve. In grade 5 PVR, 25% to 75% of the retina is detached. Grade 6 PVR is a complete retinal detachment with a prominent tractional membrane. On fundus imaging, a central hypopigmented area is seen, which corresponds with the optic nerve with a large membrane. The retina is poorly visualized as it is elevated 360° and is therefore out of focus. OCT imaging demonstrates the presence of subretinal fluid without areas of retina attachment. Histology confirms that the retina is completely detached from the underlying RPE layer, with a prominent preretinal tractional membrane.

Effects of Intravitreal Gas Injection on PVR Development

Intravitreal gas injection before RPE injection resulted in more severe PVR development when a lower number of RPE cells was injected at both 1 and 4 weeks and when a higher number of RPE cells was injected at 4 weeks (summarized in Table). After 1 week, there was a significant difference in the number of eyes that developed grade 4 or worse PVR when gas was injected before 1×10^4 RPE cells ($P = 0.01$; Fig. 3). After 4 weeks, gas injection before both 1×10^4 and 5×10^4 RPE cells resulted in a significant difference in the number of eyes that developed grade 5 or higher PVR ($P = 0.01$ and 0.03, respectively; Fig. 3). Importantly, none of the control eyes injected with gas and PBS ($n = 15$) or only injected with PBS ($n = 5$) developed any characteristics of PVR (all grade 0; Fig. 3).

Table. Gas Injection Before RPE Cell Injection

	PVR ≥ Grade 4	*P* Value
1 week after RPE		
No gas/1×10^4 RPE	0/11 (0%)	0.02
SF_6 gas/1×10^4 RPE	5/13 (38%)	
No gas/5×10^4 RPE	5/12 (42%)	0.32
SF_6 gas/5×10^4 RPE	8/13 (62%)	
	PVR ≥ Grade 5	
4 weeks after RPE		
No gas/1×10^4 RPE	3/11 (27%)	0.01
SF_6 gas/1×10^4 RPE	11/14 (79%)	
No gas/5×10^4 RPE	7/13 (54%)	0.03
SF_6 gas/5×10^4 RPE	11/12 (92%)	

Gas injection before RPE cell injection resulted in significantly more severe PVR development at both 1 week and 4 weeks when 1×10^4 RPE cells were injected and at 4 weeks when 5×10^4 cells were injected. At 1 week, the PVR cutoff for analysis was grade 4 or worse and for 4 weeks it was grade 5 or worse.

Gas Facilitates the Migration of RPE Cells to the Retina Surface

Injection of the gas promotes detachment of the posterior vitreous, which allows for the cells to migrate more rapidly to the inner retinal surface. Indeed, we see through histologic analysis that, at 1 week after RPE injection, eyes that did not receive SF_6 gas had many cells in the vitreous, whereas those that received SF_6 gas injection had more cells along or near the surface of the inner retina (Fig. 4, top panels; observed in 5 of 5 eyes analyzed for each condition). At 4 weeks after RPE injection, eyes that were not injected with gas had more contractile membranes in the vitreous, whereas eyes that had first received gas injection had more membranes along the retina (Fig. 4, bottom panels; observed in 5 of 5 eyes analyzed for each condition). Together, these results suggest that injection of SF_6 gas helped to promote RPE cell migration to the surface of the inner retina.

PVR Membranes in Vitreous and on Retina Surface Express Fibrotic Markers

Immunohistochemical analysis of cells on the retinal surface and in the vitreous of our mouse

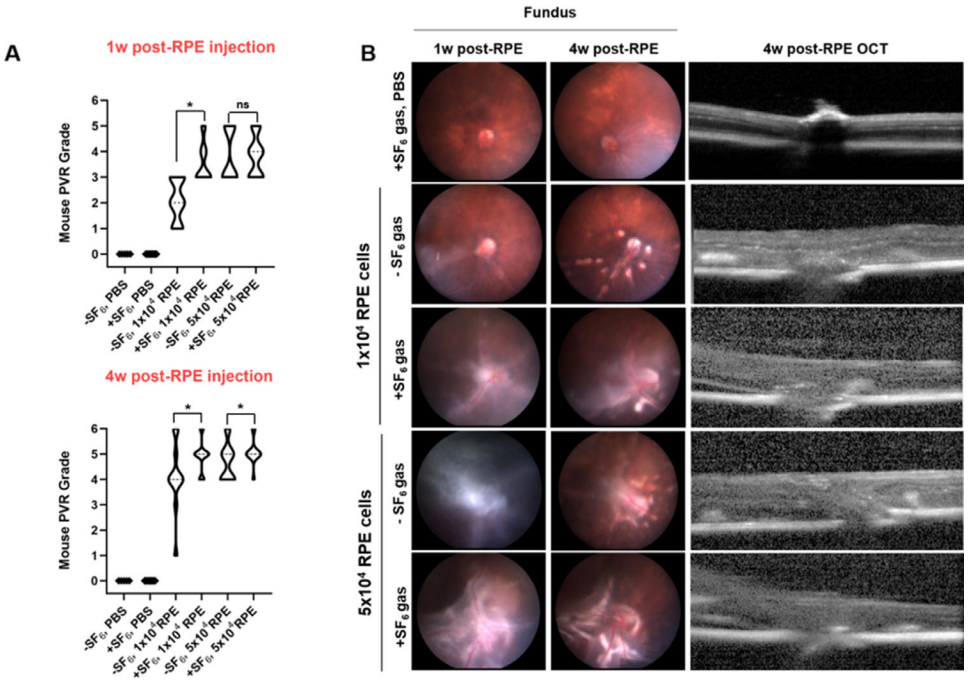

Figure 3. Intravitreal injection of SF_6 gas before RPE injection resulted in more rapid PVR development with less overall variation in PVR grades. Eyes were injected with 1×10^4 or 5×10^4 RPE cells with or without prior SF_6 gas injection, or PBS with and without gas as controls. (A) Eyes that received gas injection showed more severe PVR and less variability of PVR grade distributions at 1 week compared with eyes that did not receive a prior gas injection. At 4 weeks, there was both a higher average PVR grade and less variation in overall scores for those eyes that received the gas injection. (B) Fundus photography of representative eyes injected with gas/PBS, and 1×10^4 or 5×10^4 RPE cells with or without gas injection first at 1 and 4 weeks after RPE injection. Eyes that received the gas injection first develop more severe PVR, on average, over 4 weeks than those that just received injection of RPE cells. For each group of PVR mice, 15 eyes were injected and analyzed at 1 and 4 weeks; for PBS controls, 15 eyes were injected with gas before PBS and none developed PVR over 4 weeks. A χ^2 analysis using grade 4 or greater PVR as a cutoff for 1 week analysis and grade 5 or greater PVR for 4 week analysis. $^*P < 0.05$. ns, not significant.

PVR eyes showed that the cells that comprised the membranes along the inner retinal surface and within the vitreous expressed fibrotic markers, including alpha smooth muscle actin, fibronectin, and vimentin (Fig. 5; observed in 5 of 5 eyes analyzed for each condition). Although there is some physiologic expression of these markers within the retina, there was a clear upregulation and difference in expression patterns of these markers near the inner retinal surface and within the vitreous cavity in the mouse PVR eyes. Additionally, other cell types, including glial cells and macrophages, have been found to be components of human PVR membranes.[33,34] We also found increased expression of the glial marker glial fibrillary acidic protein and macrophage markers CD3 and CD20 in our mouse PVR membranes in the vitreous and on the inner retinal surface (Fig. 6; observed in 5 of 5 eyes analyzed for each condition). Together, these results show the RPE cells injected our mouse eye have undergone EMT and the contractile matrices of cells present both in the vitreous and along the retina surface are similar in composition to human PVR membranes.

Discussion

PVR is a condition that arises in 5% to 10% of patients after retinal detachment repair surgery and can lead to blindness.[2] RPE cells that have migrated into the vitreous and onto the inner retinal surface are exposed to growth factors and cytokines and undergo EMT to contractile fibrotic cells. It is the contraction of these PVR membranes that results in subsequent retinal detachment, damaging the photoreceptors in the process. The standard treatment for PVR is surgery to remove the membranes or remove some retinal tissue to reattach the retina.[2,3] PVR is associated with poor visual outcomes.[2,3] There are currently no pharmacologic agents approved to prevent or treat PVR. Animal models of disease processes are essential to understanding disease pathogenesis and studying the ability of candidate pharmacologic agents to prevent or treat diseases. Mouse models in particular provide the ability to study various aspects of disease pathways and pharmacologic agent mechanism using

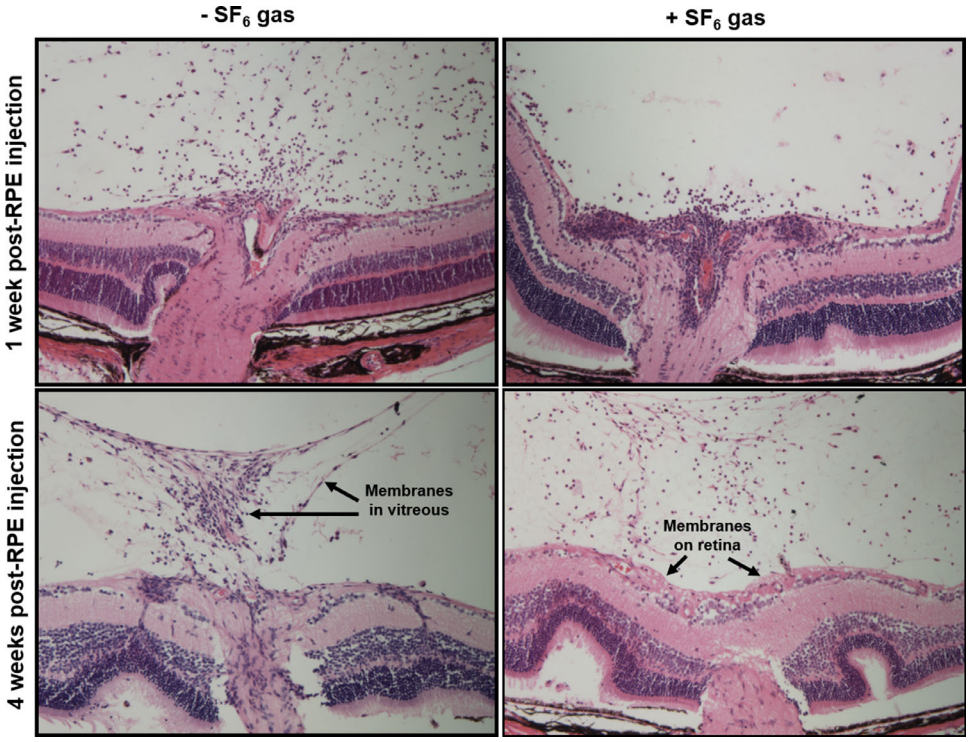

Figure 4. Intravitreal gas injection resulted in migration of RPE cells to the inner retinal surface. Injection of SF_6 gas followed by injection of 1×10^4 RPE cells promoted RPE cells migration to the blood vessels and inner retinal surface, whereas eyes that received no gas injection had more RPE cells in the vitreous 1 week after RPE injection (*top*). At 4 weeks after RPE injection, those eyes that received no gas injection had more membranes in the vitreous cavity, whereas those that received gas injection had more contractile membranes on the surface of the retina (*bottom*). Images are representative of five eyes from each experimental condition.

genetically modified animals. A reproducible mouse PVR model that recapitulates key aspects of PVR pathology without compromising retinal integrity can potentially help to provide a platform for furthering our understanding of PVR pathogenesis and testing candidate agents that inhibit or treat PVR.

In this study, we present a new mouse model of PVR induction adapted from a technique used in rabbits in which intravitreal gas followed by RPE cell injections mimic several key pathologic features of human PVR, including RPE cell migration and EMT, contraction of preretinal and vitreous membranes, and resultant retinal traction and detachments. Using fundus photography, OCT, and histologic analysis, we demonstrated the ability to induce highly reproducible PVR phenotypes in the mouse eye (Fig. 1). Based on these findings, a PVR grading scale that is specific to the mouse eye was created to distinguish the severity of PVR findings and provide the ability to quantitatively compare PVR severity (Fig. 2). This PVR grading scheme was applied in the current study to assess differences in the rapidity and severity of PVR development when comparing the impact of intravitreal gas injections before RPE cell injection (Fig. 3). In other PVR animal models, the timing of PVR development and overall severity is correlated with the concentration of cells injected into the vitreous.[18] In the current study, we found that the concentration of RPE cells injected had a mild impact on the severity of PVR. Of note, there was a high rate of severe PVR formation in both RPE cell concentration groups. It is possible that a difference with prior intravitreal SF_6 gas injection would be apparent with injections of lower concentrations of RPE cells.

Future studies using this model can use the PVR grading scale to study the efficacy of candidate therapeutic agents and their ability to inhibit the development of PVR. Additionally, the rapidity and severity of PVR development can be compared between wild-type mice and mice with specific genetic mutations associated with PVR development or in mice with overexpression or knockout of potential regulators of PVR (e.g., tumor necrosis factor α).

In humans, posterior vitreous detachments are associated with aging and are often a precursor to retinal detachment.[35] We have demonstrated the induction of a posterior vitreous detachment using an intravitreal injection of SF_6 gas results in more severe PVR

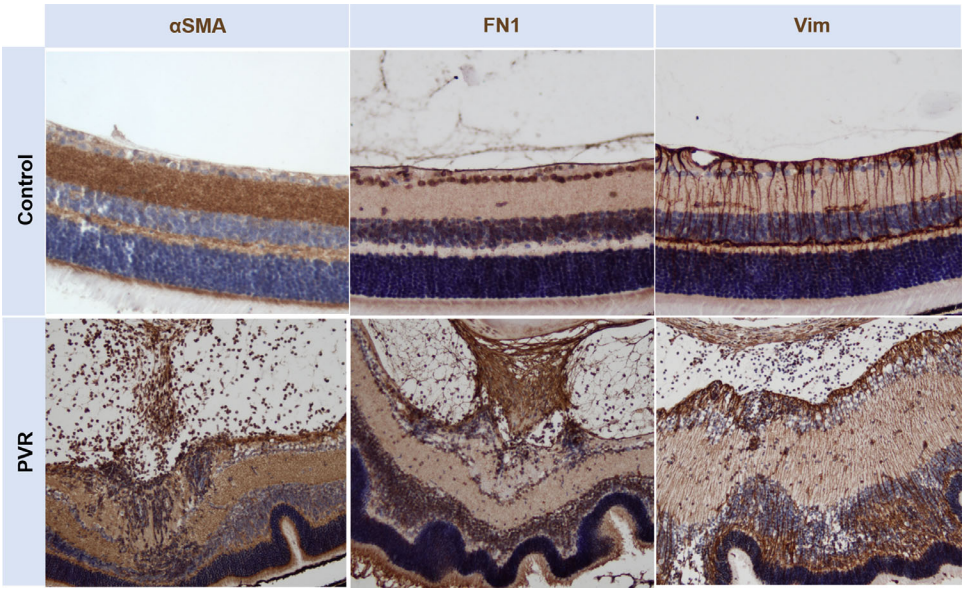

Figure 5. Preretinal and vitreous membranes express EMT markers. RPE cells that have undergone EMT to contractile, fibrotic cells express markers known to be upregulated in differentiated fibroblasts, including alpha smooth muscle actin (α-SMA), fibronectin (FN1), and vimentin (Vim), which are seen with brown staining. Compared with control eyes, mouse eyes that develop PVR and have contractile membranes on the retinal surface and in the vitreous express these makers of EMT. Images are representative of five eyes from each experimental condition.

formation (Fig. 3). One way in which a posterior vitreous detachment may promote PVR formation is that it allows for easier cell migration to the inner retina surface and allows for important cell-to-cell interactions to occur, which may otherwise be dampened by the vitreous. We are clearly able to show that injection of SF_6 gas promotes faster migration of RPE cells to the inner retina surface and favors the formation of contractile membranes on the surface of the retina (Fig. 4). Importantly, these contractile membranes that form on the retinal surface after RPE cell injection highly resemble human PVR membranes, because they stain positive for expression of the fibrotic markers alpha smooth muscle actin, fibronectin, and vimentin (Fig. 5). All of these markers have been identified in human PVR membranes and are upregulated in the samples from patients with PVR.[36] We also find the recruitment of other cells types, including macrophages and glial cells to the PVR membranes (Fig. 6). These cells have been found in human PVR membranes as well.[36] All together, these results show that we are able to initiate and monitor PVR development in the mouse eye, and that the phenotypes and membranes observed in the vitreous and retina are similar to those seen in human PVR.

Although our model replicates many aspects of PVR pathology, including RPE cell migration and EMT to fibrotic cells that induce traction on the retina resulting in retinal folds and detachments, this model also has potential limitations. In humans, retinal tears provide a point of entry for RPE cells into the vitreous cavity and precede retinal detachments and PVR development.[4,7] In our model, we consistently observe retinal detachments in our PVR eyes, but they are only secondary to injection of RPE cells and the subsequent development of tractional membranes. Although others have reported methods to induce retinal detachment in the mouse eye,[37,38] these models do not consistently result in a retinal tear. Our model likely accelerates the PVR process, compared with the time course of PVR development in humans, by injecting a large number of RPE cells directly into the vitreous cavity. However, depending on the number of RPE cells injected, our model can show very fast development of high-grade PVR or a slower progression to high-grade PVR over many weeks. Of note, a risk factor for PVR development is a giant retinal tear, which can potentially result in a greater number of RPE cells being dispersed in the vitreous.[39]

One other limitation to this model is that we inject human RPE cells, which may result in some degree of inflammation from the presence of foreign cells. Of note, other investigators have injected RPE cells from both humans[16] and nongenetically identical rabbits[14] into the commonly used rabbit PVR model and shown the development of PVR; both of these types of foreign cells would be expected to generate a degree of inflammation as well. We chose to use ARPE-19 cells owing to their ease of availability in large numbers and, because

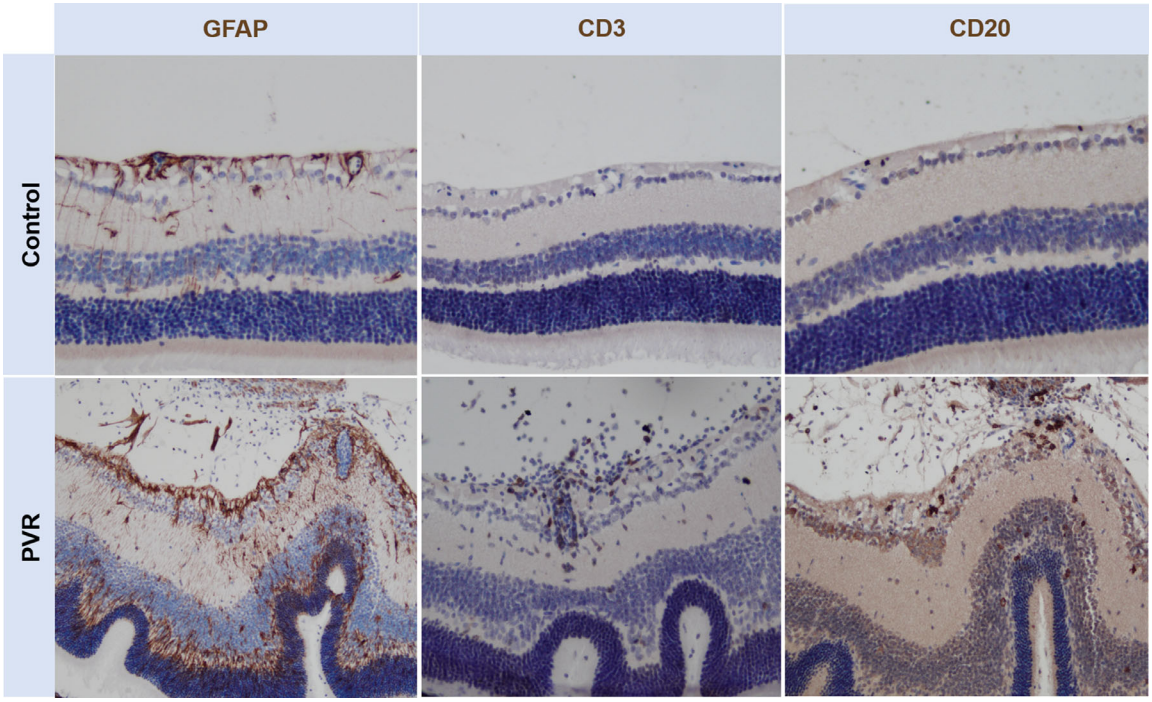

Figure 6. Preretinal and vitreous membranes express markers of other cellular components of PVR membranes. In addition to RPE cells, PVR membranes are comprised glial cells and macrophages. Compared with control eyes, mouse PVR eyes have increased levels of expression of the glial marker glial fibrillary acidic protein along the retinal surface and in the vitreous (brown staining). CD3 (a marker of T cells) and CD20 (a marker of B cells) are also both present along the inner retinal surface and in the contractile membranes of the vitreous (*brown staining*). Images are representative of five eyes from each experimental condition.

the cells are immortalized, we expect little variation from different passages, which would limit variability.[40] Additionally, inflammation is a key characteristic of PVR and inflammatory cytokines are present in the vitreous of patients with PVR.[4,41] Of note, another group has used intravitreal injection of ARPE-19 cells without gas to study the role of Notch signaling in PVR in the mouse eye.[14,41]

In summary, we have presented a novel mouse model of PVR that combines gas injection to promote vitreous detachment, followed by intravitreal injection of RPE cells. This model is able to reproduce many aspects of human PVR pathogenesis and results in the development of a reproducible PVR phenotype with preretinal tractional membranes and retinal detachments. Although similar models have been developed in the rabbit, a mouse model allows for genetic manipulations, including looking at the role of certain genes and pathways and their role in PVR development. Additionally, potential pharmacologic agents for preventing and treating PVR can more easily tested with a larger number of animals when using a mouse model, compared with a rabbit model, owing to practical factors such as cost and space. We are hopeful that this mouse model of PVR will provide a platform to advance research in PVR, both on the pharmacologic and molecular levels.

Acknowledgments

We thank Olivia Marola for her teaching of intravitreal mouse injections, and Jacob Proano, Mohammad Bawany, Elisa Roztocil, and Christine Hammond for their insightful discussions and comments. We also thank Charles Pfeifer and Jesse Schallek for their help and expertise in OCT imaging.

This work was funded by Research to Prevent Blindness Unrestricted Grant (to the Flaum Eye Institute) and NIHP30EY001319 (David Williams, Center for Visual Sciences).

Disclosure: **A. Heffer**, None; **V. Wang**, None; **J. Sridhar**, None; **S.E. Feldon**, None; **R.T. Libby**, None; **C.F. Woeller**, None; **A.E. Kuriyan**, None

* CFW and AEK are co-senior authors.

References

1. Tseng W, Cortez RT, Ramirez G, Stinnett S, Jaffe GJ. Prevalence and risk factors for proliferative vitreoretinopathy in eyes with rhegmatogenous retinal detachment but no previous vitreoretinal surgery. *Am J Ophthalmol*. 2004;137:1105–1115, doi:10.1016/j.ajo.2004.02.008.
2. Cardillo JA, Stout JT, LaBree L, et al. Posttraumatic proliferative vitreoretinopathy. The epidemiologic profile, onset, risk factors, and visual outcome. *Ophthalmology*. 1997;104:1166–1173.
3. Abrams GW, Azen SP, McCuen BW, Flynn HW, Lai MY, Ryan SJ. Vitrectomy with silicone oil or long-acting gas in eyes with severe proliferative vitreoretinopathy: results of additional and long-term follow-up. Silicone Study report 11. *Arch Ophthalmol*. 1997;115:335–344.
4. Pennock S, Haddock LJ, Eliott D, Mukai S, Kazlauskas A. Is neutralizing vitreal growth factors a viable strategy to prevent proliferative vitreoretinopathy? *Prog Retin Eye Res*. 2014;40:16–34, doi:10.1016/j.preteyeres.2013.12.006.
5. Anderson DH, Stern WH, Fisher SK, Erickson PA, Borgula GA. The onset of pigment epithelial proliferation after retinal detachment. *Invest Ophthalmol Vis Sci*. 1981;21:10–16.
6. Kiilgaard JF, Prause JU, Prause M, Scherfig E, Nissen MH, la Cour M. Subretinal posterior pole injury induces selective proliferation of RPE cells in the periphery in in vivo studies in pigs. *Invest Ophthalmol Vis Sci*. 2007;48:355–360, doi:10.1167/iovs.05-1565.
7. Idrees S, Sridhar J, Kuriyan AE. Proliferative vitreoretinopathy: a review. *Int Ophthalmol Clin*. 2019;59:221–240, doi:10.1097/IIO.0000000000000258.
8. Hiscott PS, Grierson I, McLeod D. Retinal pigment epithelial cells in epiretinal membranes: an immunohistochemical study. *Br J Ophthalmol*. 1984;68:708–715.
9. Hiscott P, Sheridan C, Magee RM, Grierson I. Matrix and the retinal pigment epithelium in proliferative retinal disease. *Prog Retin Eye Res*. 1999;18:167–190.
10. Grierson I, Hiscott PS, Hitchins CA, McKechnie NM, White VA, McLeod D. Which cells are involved in the formation of epiretinal membranes? *Semin Ophthalmol*. 1987;2:99–109, doi:10.3109/08820538709062514.
11. Agrawal RN, He S, Spee C, Cui JZ, Ryan SJ, Hinton DR. In vivo models of proliferative vitreoretinopathy. *Nat Protoc*. 2007;2:67–77, doi:10.1038/nprot.2007.4.
12. Cleary PE, Ryan SJ. Method of production and natural history of experimental posterior penetrating eye injury in the rhesus monkey. *Am J Ophthalmol*. 1979;88:216–220, doi:10.1016/0002-9394(79)90468-9.
13. Wilson CA, Khawly JA, Hatchell DL, Machemer R. Experimental traction retinal detachment in the cat. *Graefes Arch Clin Exp Ophthalmol*. 1991;229:568–573, doi:10.1007/bf00203323.
14. Radtke ND, Tano Y, Chandler D, Machemer R. Simulation of massive periretinal proliferation by autotransplantation of retinal pigment epithelial cells in rabbits. *Am J Ophthalmol*. 1981;91:76–87, doi:10.1016/0002-9394(81)90352-4.
15. Fastenberg DM, Diddie KR, Sorgente N, Ryan SJ. A comparison of different cellular inocula in an experimental model of massive periretinal proliferation. *Am J Ophthalmol*. 1982;93:559–564. doi:10.1016/s0002-9394(14)77369-6.
16. Wong CA, Potter MJ, Cui JZ, et al. Induction of proliferative vitreoretinopathy by a unique line of human retinal pigment epithelial cells. *Can J Ophthalmol*. 2002;37:211–220.
17. Zhang J, Yuan G, Dong M, et al. Notch signaling modulates proliferative vitreoretinopathy via regulating retinal pigment epithelial-to-mesenchymal transition. *Histochem Cell Biol*. 2017;147:367–375, doi:10.1007/s00418-016-1484-x.
18. Hida T, Chandler DB, Sheta SM. Classification of the stages of proliferative vitreoretinopathy in a refined experimental model in the rabbit eye. *Graefes Arch Clin Exp Ophthalmol*. 1987;225:303–307.
19. Chandler DB, Quansah FA, Hida T, Machemer R. A refined experimental model for proliferative vitreoretinopathy. *Graefes Arch Clin Exp Ophthalmol*. 1986;224:86–91, doi:10.1007/bf02144144.
20. Hardwick C, Feist R, Morris R, et al. Tractional force generation by porcine Müller cells: stimulation by growth factors in human vitreous. *Invest Ophthalmol Vis Sci*. 1997;38:2053–2063.
21. Vergara O, Ogden T, Ryan S. Posterior penetrating injury in the rabbit eye: effect of blood and ferrous ions. *Exp Eye Res*. 1989;49:1115–1126, doi:10.1016/s0014-4835(89)80030-2.
22. Hui YN, Goodnight R, Sorgente N, Ryan SJ. Fibrovascular proliferation and retinal detachment after intravitreal injection of activated macrophages in the rabbit eye. *Am J Ophthalmol*. 1989;108:176–184, doi:10.1016/0002-9394(89)90014-7.
23. Sakamoto T, Kimura H, Scuric Z, et al. Inhibition of experimental proliferative vitreoretinopathy by

retroviral vector-mediated transfer of suicide gene. Can proliferative vitreoretinopathy be a target of gene therapy? *Ophthalmology*. 1995;102:1417–1424, doi:10.1016/s0161-6420(95)30850-0.
24. Kuriyama S, Ohuchi T, Yoshimura N, Honda Y, Hiraoka M, Abe M. Evaluation of radiation therapy for experimental proliferative vitreoretinopathy in rabbits. *Graefes Arch Clin Exp Ophthalmol*. 1990;228:552–555, doi:10.1007/bf00918489.
25. Kuo H-K, Chen Y-H, Kuo Y-H, Ke M-C, Tseng Y-C, Wu P-C. Evaluation of the effect of everolimus on retinal pigment epithelial cells and experimental proliferative vitreoretinopathy. *Curr Eye Res*. 2018;43:333–339, doi:10.1080/02713683.2017.1396618.
26. Chen H, Wang H, An J, Shang Q, Ma J. Inhibitory effects of plumbagin on retinal pigment epithelial cell epithelial-mesenchymal transition in vitro and in vivo. *Med Sci Monit*. 2018;24:1502–1510, doi:10.12659/msm.906265.
27. Skeie JM, Mahajan VB. Proteomic interactions in the mouse vitreous-retina complex. *PLoS One*. 2013;8:e82140, doi:10.1371/journal.pone.0082140.
28. Cantó Soler MV, Gallo JE, Dodds RA, Suburo AM. A mouse model of proliferative vitreoretinopathy induced by dispase. *Exp Eye Res*. 2002;75:491–504, doi:10.1006/exer.2002.2031.
29. Gao Q, Wang W, Lan Y, et al. The inhibitory effect of small interference RNA protein kinase C-alpha on the experimental proliferative vitreoretinopathy induced by dispase in mice. *Int J Nanomedicine*. 2013;8:1563–1572, doi:10.2147/IJN.S37635.
30. Márkus B, Pató Z, Sarang Z, et al. The proteomic profile of a mouse model of proliferative vitreoretinopathy. *FEBS Open Bio*. 2017;7:1166–1177, doi:10.1002/2211-5463.12252.
31. Yoo K, Son BK, Kim S, Son Y, Yu S-Y, Hong HS. Substance P prevents development of proliferative vitreoretinopathy in mice by modulating TNF-α. *Mol Vis*. 2017;23:933–943.
32. Kaplan HJ, Chiang C-W, Chen J, Song S-K. Vitreous volume of the mouse measured by quantitative high-resolution MRI. *Invest Ophthalmol Vis Sci*. 2010;51:4414–4414.
33. Sramek SJ, Wallow IH, Stevens TS, Nork TM. Immunostaining of preretinal membranes for actin, fibronectin, and glial fibrillary acidic protein. *Ophthalmology*. 1989;96:835–841, doi:10.1016/s0161-6420(89)32817-x.
34. Limb GA, Chignell AH, Woon H, Green W, Cole CJ, Dumonde DC. Evidence of chronic inflammation in retina excised after relaxing retinotomy for anterior proliferative vitreoretinopathy. *Graefes Arch Clin Exp Ophthalmol*. 1996;234:213–220, doi:10.1007/bf00430412.
35. Sebag J. Age-related changes in human vitreous structure. *Graefes Arch Clin Exp Ophthalmol*. 1987;225:89–93, doi:10.1007/bf02160337.
36. Asato R, Yoshida S, Ogura A, et al. Comparison of gene expression profile of epiretinal membranes obtained from eyes with proliferative vitreoretinopathy to that of secondary epiretinal membranes. *PLoS One*. 2013;8:e54191, doi:10.1371/journal.pone.0054191.
37. Matsumoto H, Miller JW, Vavvas DG. Retinal detachment model in rodents by subretinal injection of sodium hyaluronate. *J Vis Exp*. 2013;79:50660, doi:10.3791/50660.
38. Saika S, Yamanaka O, Nishikawa-Ishida I, et al. Effect of Smad7 gene overexpression on transforming growth factor beta-induced retinal pigment fibrosis in a proliferative vitreoretinopathy mouse model. *Arch Ophthalmol*. 2007;125:647–654, doi:10.1001/archopht.125.5.647.
39. Chang S, Lincoff H, Zimmerman NJ, Fuchs W. Giant retinal tears: surgical techniques and results using perfluorocarbon liquids. *Arch Ophthalmol*. 1989;107:761–766, doi:10.1001/archopht.1989.01070010779046.
40. Dunn KC, Aotaki-Keen AE, Putkey FR, Hjelmeland LM. ARPE-19, a human retinal pigment epithelial cell line with differentiated properties. *Exp Eye Res*. 1996;62:155–169, doi:10.1006/exer.1996.0020.
41. Limb GA, Little BC, Meager A, et al. Cytokines in proliferative vitreoretinopathy. *Eye (Lond)*. 1991;5(Pt 6):686–693, doi:10.1038/eye.1991.126.
42. Zhang J, Zhou Q, Yuan G, Dong M, Shi W. Notch signaling regulates M2 type macrophage polarization during the development of proliferative vitreoretinopathy. *Cell Immunol*. 2015;298:77–82, doi:10.1016/j.cellimm.2015.09.005.